



Factors impacting the efficacy of the in-situ vaccine with CpG and OX40 agonist

Alexander A. Pieper¹ · Dan V. Spiegelman¹ · Mildred A. R. Felder¹ · Arika S. Feils¹ · Noah W. Tsarovsky¹ · Jen Zaborek² · Zachary S. Morris¹ · Amy K. Erbe¹ · Alexander L. Rakhmievich¹ · Paul M. Sondel^{1,3,4}

Received: 30 September 2022 / Accepted: 22 March 2023 / Published online: 5 April 2023
© The Author(s) 2023

Abstract

Background The *in-situ* vaccine using CpG oligodeoxynucleotide combined with OX40 agonist antibody (CpG + OX40) has been shown to be an effective therapy activating an anti-tumor T cell response in certain settings. The roles of tumor volume, tumor model, and the addition of checkpoint blockade in the efficacy of CpG + OX40 *in-situ* vaccination remains unknown.

Methods Mice bearing flank tumors (B78 melanoma or A20 lymphoma) were treated with combinations of CpG, OX40, and anti-CTLA-4. Tumor growth and survival were monitored. In vivo T cell depletion, tumor cell phenotype, and tumor infiltrating lymphocyte (TIL) studies were performed. Tumor cell sensitivity to CpG and macrophages were evaluated in vitro.

Results As tumor volumes increased in the B78 (one-tumor) and A20 (one-tumor or two-tumor) models, the anti-tumor efficacy of the *in-situ* vaccine decreased. In vitro, CpG had a direct effect on A20 proliferation and phenotype and an indirect effect on B78 proliferation via macrophage activation. As A20 tumors progressed in vivo, tumor cell phenotype changed, and T cells became more involved in the local CpG + OX40 mediated anti-tumor response. In mice with larger tumors that were poorly responsive to CpG + OX40, the addition of anti-CTLA-4 enhanced the anti-tumor efficacy in the A20 but not B78 models.

Conclusions Increased tumor volume negatively impacts the anti-tumor capability of CpG + OX40 *in-situ* vaccine. The addition of checkpoint blockade augmented the efficacy of CpG + OX40 in the A20 but not B78 model. These results highlight the importance of considering multiple preclinical model conditions when assessing the efficacy of cancer immunotherapy regimens and their translation to clinical testing.

Keywords In-situ vaccine · CpG · OX40 agonist · Anti-CTLA-4 · Preclinical tumor progression

Introduction

Emerging clinical evidence indicates patients with greater tumor burden have reduced responses to immune checkpoint blockade (ICB) [1–3]. Some preclinical data demonstrate that larger tumor burdens are more immunosuppressive at baseline [4–6], and these baseline characteristics contribute to larger tumors being less responsive to ICB and other immunotherapy strategies [4, 7–9]. However, other reports demonstrate that anti-tumor efficacy of immunotherapy either did not correlate with [10] or improved with increased tumor burden [11]. We have previously published the effects of immunocytokines (ICs, tumor antigen specific antibodies linked to stimulatory cytokines) as *in-situ* vaccines in various preclinical models [7, 12–14]. In the NXS2 neuroblastoma model [7], intratumoral (IT) injections of a GD2 targeted IC significantly improved survival over control mice

✉ Paul M. Sondel
pmsondel@humonc.wisc.edu

¹ Department of Human Oncology, School of Medicine and Public Health, University of Wisconsin, Madison, WI, USA

² Department of Biostatistics and Medical Informatics, School of Medicine and Public Health, University of Wisconsin, Madison, WI, USA

³ Department of Pediatrics, School of Medicine and Public Health, University of Wisconsin, Madison, WI, USA

⁴ 4159 MACC Fund UW Childhood Cancer Research Wing, Wisconsin Institute for Medical Research, University of Wisconsin, 1111 Highland Avenue, Madison, WI 53705-2275, USA

if tumors were less than 34 mm³ but not if tumor volumes were greater than 34 mm³. The relationship between tumor volume, efficacy, and mechanism of *in-situ* vaccines has not been fully characterized.

The combination of CpG oligodeoxynucleotide and OX40 agonist antibody (CpG + OX40) can activate a potent *in-situ* vaccine effect in the preclinical A20 B-cell lymphoma model [15–17]. IT injections of CpG + OX40 can cure mice of both a treated tumor and distant untreated tumor in a T cell dependent manner [17]. CpG is a pathogen associated molecular pattern (PAMP) molecule that activates toll like receptor 9 (TLR-9) in macrophages, dendritic cells, and natural killer cells [18]. The OX40 molecule is a costimulatory receptor expressed by T cells after T cell receptor (TCR) engagement [19]. When activated, OX40 provides a “second signal” for T cell activation [19–21]. OX40 activation on T regulatory cells (Tregs) can lead to Treg apoptosis, decreased production of interleukin (IL)-10, and decreased FoxP3 expression [22–24]. In the A20 model, we and others have shown IT injections of CpG can increase OX40 expression on CD4 + effector and CD8 + T cells in the tumor microenvironment (TME) [17, 25].

In this report, we tested how tumor volume and tumor model influenced the anti-tumor efficacy and mechanism of the *in-situ* vaccine CpG + OX40 in two preclinical tumor types where clinical IT injections are clinically achievable due to tumor accessibility. As tumors progress, CpG + OX40 lost effectiveness in the B78 melanoma and A20 lymphoma models. In vitro macrophage co-culture experiments suggested that CpG is functioning differently in the B78 and A20 models to slow tumor progression. As untreated A20 tumors became larger in vivo, tumor phenotypic changes occurred, which correlated with the blunted effect of the T cell mediated *in-situ* vaccine. T cell depletion studies in mice bearing two separate A20 tumors demonstrated different T cell requirements for a local anti-tumor response to CpG + OX40 depending on the starting volumes of the two tumors. Finally, in conditions that were unresponsive to CpG + OX40 alone, the addition of anti-CTLA-4 restored the tumor curing ability of CpG + OX40 in A20-bearing mice, but not B78-bearing mice.

Methods

Mice

Female *C57BL/6* and *Balb/c* 6–8 week old mice were purchased from Taconic Biosciences (Rensselaer, NY) and housed in accordance with the Guide for Care and Use of Laboratory Mice. Experiments were performed under an institutional animal care and use committee approved animal protocol in accordance with NIH guidelines. Per our

institutionally approved protocol, mice were euthanized when any tumor size reached 20 mm in the longest dimension or when they showed substantial systemic effects of the enlarging tumor.

Cell culture

A20 lymphoma was obtained from Dr. Stephen Gillies in 2017. To achieve consistent tumor engraftment, A20 cells were passaged in vivo as previously described [25]. B78-D14 (B78) melanoma was obtained from Dr. Ralph Reisfeld in 2002. B78 and A20 cells were cultured as previously described [25].

In vivo tumor models

A20 (5×10^6) and B78 (2×10^6) cells were injected intradermally into the right and/or left flank of *Balb/c* mice (A20) and *C57BL/6* mice (B78). Tumors were measured twice per week, and tumor volumes were calculated as previously described [14]. Once tumor volumes reached target size, mice were randomized to have similar average starting tumor volumes for the tumor scheduled to receive IT treatment. Tumor volumes were categorized as follows: first-palpable (~ 15 mm³), small (~ 100 mm³), moderate (~ 200 mm³), large (~ 350 mm³), and advanced (~ 1000 mm³). B78 tumor volumes reached first palpable (~ 15 mm³) and small (~ 100 mm³) sizes 10 days and 21 days after tumor cell injection. A20 tumor volumes reached small (~ 100 mm³), moderate (~ 200 mm³), large (~ 350 mm³), and advanced (~ 1000 mm³) sizes 8, 14, 18, and 24 days after tumor cell injections. Mice were randomized at these time points (± 1 day) after tumor cell injections for the given experiments. Mice were euthanized when the greatest tumor dimension reached 20 mm or, specifically in the A20 model, the mouse became moribund due to metastatic disease. A complete response (CR) was defined as complete resolution of all detectable tumor(s). In mice with 2 tumors, a local complete response (LCR) was defined as complete resolution of tumor at the local site (either the treated or untreated tumor). Cure is defined as complete resolution of all tumor(s) in an individual animal that was maintained, without any sign of recurrent tumor, until the end of the monitoring period (normally 90 days).

Immunotherapy and antibodies

CpG (50 μ g; 1826 from Integrated DNA Technologies) and anti-OX40 (20 μ g; OX86 clone, European Collection of Cell Cultures, harvested and isolated from immunodeficient mice [26]) in 60 μ L PBS were injected IT with a 29½ gauge insulin syringe on days 0, 2, and 4 after randomization. Anti-CTLA-4 (200 μ g in 100 μ L PBS; clone 9D9 from Bristol Myers Squibb) was injected intraperitoneally (IP) with a 26

gauge needle on days 2, 5, and 8. Anti-CD4 (400 µg; clone GK1.5 from Bio X Cell) and anti-CD8 (400 µg; clone 2.43 from Bio X Cell) in 200 µL PBS were injected IP on days – 1, 6, and 13 for T cell depletion experiments [27].

The antibodies used for flow cytometry analysis are listed in Table S1.

Tumor cell and tumor infiltrating immune cell analysis

B78 tumors were grown as described above. A20 tumors were grown by injecting 5×10^6 (large) or 1×10^6 (small) A20 cells. Once tumors reached target volumes, mice were randomized, treated, and tumors were harvested and prepped as described [25, 27]. Brilliant stain buffer (BD Biosciences) and the FoxP3/Transcription Factor Staining Buffer Set (eBioscience) were used per manufacturer instructions. TLR-9 expression on cultured tumor cells was determined as described [28].

All data were collected on an Attune flow cytometer (ThermoFisher) and analyzed with FlowJo v10 software (BD). Tregs were defined as CD45 + /CD3 + /CD4 + /CD25 + /FoxP3 + ; CD4 + cells not CD25 + and FoxP3 + double positive were defined as non-regulatory CD4 + T cells.

Macrophage anti-tumor effect in vitro

Murine peritoneal exudate cells were obtained by peritoneal lavage and plastic adhesion, as described [28]. Adhesion-purified macrophages from *C57BL/6* or *Balb/c* mice were incubated with B78 or A20 tumor cells (1×10^4 per well) for 48 h in medium with or without CpG (5 or 50 µg/ml), and a [³H]thymidine incorporation assay was performed [28]. Results are expressed as counts per 5 min for triplicate wells ± standard error of the mean (SEM). Macrophages alone (in the absence of tumor cells or CpG) incorporated negligible amounts of [³H]thymidine [28].

Statistical analysis

Average group tumor volumes are plotted showing mean ± SEM. Tumor volume plots were summarized by time-weighted average (area under the volume-time curve, calculated using trapezoidal method). Time-weighted averages were compared between treatment groups overall by Kruskal–Wallis tests. If significant by Kruskal–Wallis test, pairwise comparisons were conducted using Mann–Whitney tests. Survival data were plotted using Kaplan–Meier methods and analyzed using log-rank comparisons. Flow cytometry results are plotted as mean ± SEM, with each symbol representing results from one mouse/sample. Flow cytometry data were analyzed via Mann–Whitney tests (when comparing two groups) or

one-way ANOVA with Tukey’s multiple comparison corrections (when comparing three or more groups). Complete response rates were analyzed overall with chi-square tests (when comparing three or more groups). If significant by chi-square tests, pairwise comparisons were conducted using two-sample tests of proportions. [³H]thymidine results are plotted as mean ± SEM fold change differences comparing wells of a particular experiment and macrophage condition to the intra-experimental media average. Experimental fold change differences were analyzed via two-way ANOVA with Tukey’s multiple comparison corrections. *P* values < 0.05 were considered significant and were indicated in all figures as follows: **P* ≤ 0.05; ***P* ≤ 0.01; ****P* ≤ 0.001; *****P* ≤ 0.0001; ns—nonsignificant. Each tumor volume experiment shown was repeated at least once.

Results

CpG + OX40 cures mice of first-palpable B78 melanomas but fails to control growth of small B78 melanomas

We initially tested the anti-tumor capability of CpG + OX40 in the immunologically cold B78 model when tumors were first-palpable (~ 15 mm³). At this size, CpG + OX40 demonstrated a significant anti-tumor effect, curing 7 of 10 mice, and significantly improving survival over control mice (Fig. 1a, b, e). Next, we tested the anti-tumor efficacy of CpG + OX40 in small (~ 100 mm³) B78 tumors. Unlike ~ 15 mm³ B78 tumors, ~ 100 mm³ B78 tumors showed no significant anti-tumor response to CpG + OX40 (Fig. 1c). The survival benefit provided by CpG + OX40 in first-palpable B78 tumors was lost in the small B78 model (Fig. 1d), and no mice were cured of their tumor (Fig. 1e).

Flow cytometry analyses were performed on untreated small (~ 100 mm³) and large (~ 350 mm³) B78 tumors to explore if there were baseline immunologic or tumor phenotype differences as B78 tumors progress in size. No significant baseline TIL or tumor phenotype differences were measured (Fig. S1A–C). Significantly fewer live tumor cells (GD2 + cells) per total events were counted in large tumors compared to small tumors, suggesting increased levels of tumor necrosis as B78 tumors progress (Fig. S1D). In separate flow experiments, CpG + OX40 treatment significantly lowered the Treg/CD45 + ratio in the TME of small B78 tumors (Fig. S1E).

CpG + OX40 cures mice of moderate and large A20 lymphoma tumors but fails to cure in the advanced disease setting

We next demonstrated the effect of tumor size on response to CpG + OX40 in *Balb/c* mice bearing a single A20

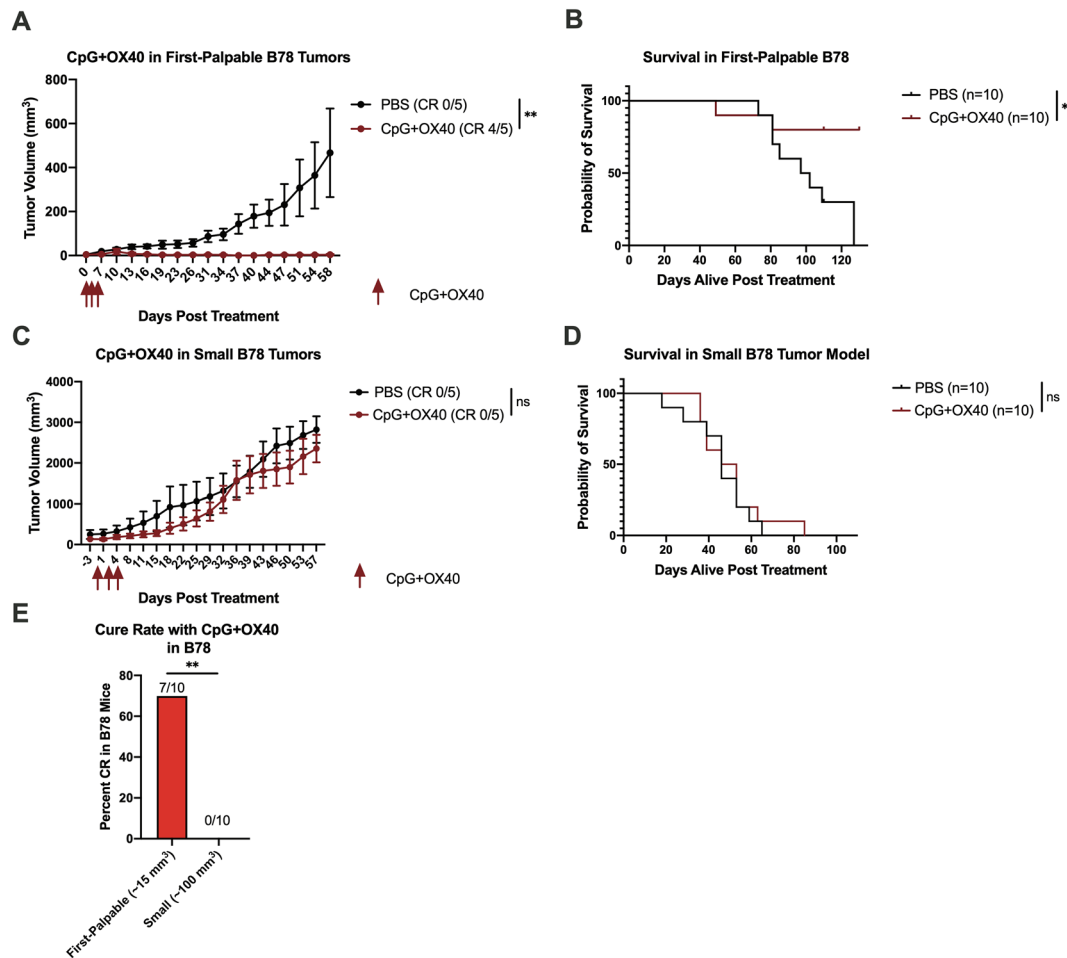


Fig. 1 CpG+OX40 *in-situ* vaccine cures mice of first-palpable ($\sim 15 \text{ mm}^3$) B78 tumors but fails to slow tumor progression of small ($\sim 100 \text{ mm}^3$) B78 Tumors. **a** Average tumor volume (\pm SEM) from a representative experiment and **b** combined overall survival from two independent experiments showing responses to PBS (black) or CpG+OX40 (red) in the first-palpable ($\sim 15 \text{ mm}^3$) B78 tumor model. **c** Average tumor volume (\pm SEM) from a representative experiment and **d** the combined overall survival from two independent experiments showing responses to PBS (black) or CpG+OX40 (red) in the

small ($\sim 100 \text{ mm}^3$) B78 model. The number of mice demonstrating a complete response (CR) in **a** and **c** is shown in parentheses. **e** The percent of mice bearing first-palpable or small B78 tumors that were cured with CpG+OX40 treatment. *P* values for tumor volume plots were calculated using time-weighted average analysis. *P* values for overall survival were calculated via log rank test. *P* value for cure rate calculated via chi-square test. **P* ≤ 0.05 ; ***P* ≤ 0.01 ; ns, not significant

tumor. In separate experiments, we compared PBS vs. CpG+OX40 in mice bearing moderate ($\sim 200 \text{ mm}^3$), large ($\sim 350 \text{ mm}^3$), or advanced ($\sim 1000 \text{ mm}^3$) A20 tumors. In mice with moderate or large A20 tumors, CpG+OX40 activated a strong anti-tumor response, causing significant tumor regression, improving survival over control, and most mice were cured of their tumor (Fig. 2a–d, g). In contrast, advanced ($\sim 1000 \text{ mm}^3$) A20 tumors treated with CpG+OX40 continued to grow progressively, though tumor growth was significantly slowed (Fig. 2e). As a result, all treated mice died (Fig. 2f). Thus, the curative potential of CpG+OX40 seen in the moderate and large A20 models was lost in the advanced model (Fig. 2g).

A20 tumor phenotype changes with size progression

To evaluate tumor phenotype changes as A20 tumors progress in size, we harvested untreated small ($\sim 150 \text{ mm}^3$) and large ($\sim 500 \text{ mm}^3$) A20 tumors for flow analysis (gating strategy presented in Fig. S2). CD19⁺ cells in large tumors demonstrated significantly lower MHC-I, MHC-II, CD80, and CD86 expression compared to small tumors (Fig. 3a–c). TIL analysis on untreated small and large A20 tumors demonstrated trends toward increased ratios of CD3⁺/CD19⁺, CD4⁺ non-Treg/CD19⁺, and CD8⁺/CD19⁺ (*p* = 0.0519, 0.126, 0.126, respectively) in small tumors compared to

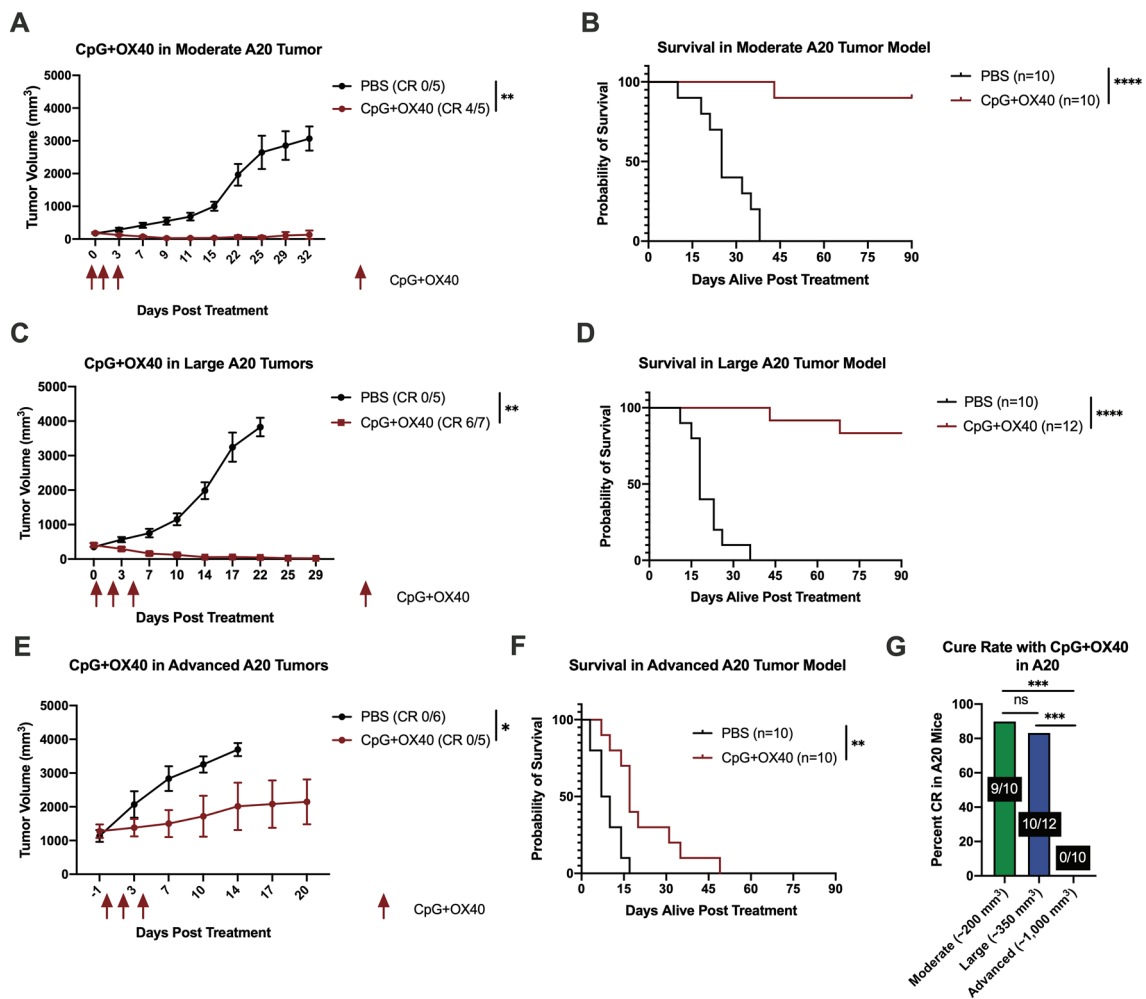


Fig. 2 Decreased Curative Effect of CpG+OX40 *In-situ* Vaccine in A20 Model as Tumor Burden Increases. **a**, **c**, **e** Average tumor volume (\pm SEM) from a representative experiment and **b**, **d**, **f** combined overall survival from two independent experiments of mice bearing a **a**, **b** moderate (~ 200 mm³), **c**, **d** large (~ 350 mm³), **e**, **f** or advanced (~ 1000 mm³) A20 flank tumor treated with PBS (black) or CpG+OX40 (red). The number of mice cured (CR), based on showing a complete response and remaining tumor-free to day 90, of their

tumor in **a**, **c**, and **e** is shown in parentheses. **g** The percent of mice bearing a single moderate (green), large (blue), or advanced (purple) A20 tumor that were cured with CpG+OX40 treatment. *P* values for tumor volume plots were calculated using time-weighted average analysis. *P* values for overall survival were calculated via log rank test. *P* value for cure rate calculated via chi-square tests. **P* ≤ 0.05 ; ***P* ≤ 0.01 ; ****P* ≤ 0.001 ; *****P* ≤ 0.0001 ; ns, not significant

large tumors (Fig. S3). There was a small but significant increase in the Treg/CD19⁺ ratio in small tumors compared to large tumors (Fig. S3).

CpG acts differently on B78 and A20 tumors: indirectly preventing B78 proliferation via macrophages, while acting directly to slow A20 cell proliferation

We were interested in what effect CpG and CpG-activated *C57BL/6* or *Balb/c* peritoneal derived macrophages had on B78 and A20 proliferation. In the absence of macrophages, CpG appeared to increase B78 proliferation though B78 cells do not express TLR-9 (Fig. S4A, B). *C57BL/6* derived

macrophages significantly slowed B78 proliferation in a dose dependent manner when activated with CpG (Fig. S4A).

Taken together, the above data suggest CpG+OX40 is functioning, in part, by activating tumor associated macrophages (Fig. S4A) and decreasing the frequency of tumor infiltrating Tregs in the B78 model (Fig. S1E). If B78 tumors are treated early, these immunologic modifications likely contribute to curing mice of their tumor burden. However if B78 tumors are allowed to progress (~ 100 mm³), the activation of macrophages and decrease of Tregs is insufficient to slow tumor progression or prolong survival.

Others have published that CpG increases immune co-stimulatory molecule expression on mouse and human B cell lymphomas *in vitro* [29, 30]. We observed similar *in vivo*

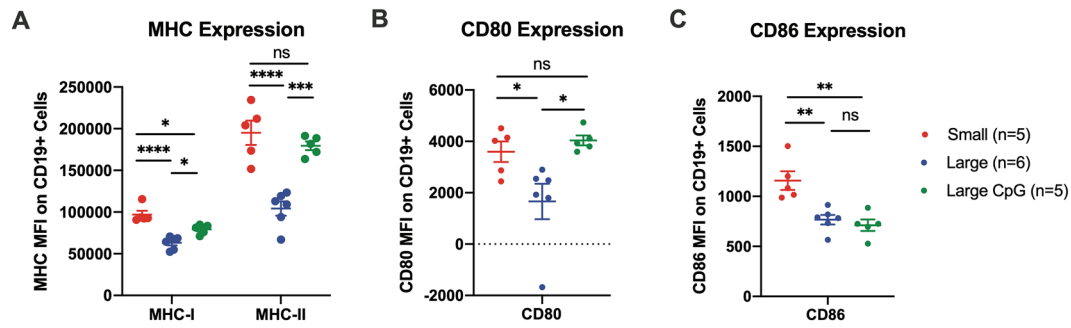


Fig. 3 In Vivo Tumor Phenotypic Changes with Tumor Progression and Intratumoral CpG. Average (\pm SEM) median fluorescent intensity (MFI) of **a** MHC-I and MHC-II, **b** CD80, and **c** CD86 on CD19+ cells (e.g. A20 tumor cells) in small (~ 150 mm³) untreated (red), large (500 mm³) untreated (blue), and large (500 mm³) CpG treated (green) A20 tumors. Large CpG treated tumors were injected

phenotypic changes on CD19+ cells 48 h after IT injection of CpG. CD19+ cells from large (~ 500 mm³) A20 tumors treated with CpG demonstrated significantly increased MHC-I, MHC-II, and CD80 expression compared to large untreated tumors (Fig. 3a, b). These phenotypic changes following CpG exposure were replicated in vitro (Fig. S4E), suggesting that CpG is acting directly on A20 cells via their confirmed TLR-9 (Fig. S4D) to modify tumor cell phenotype.

To compare the CpG effects on A20 cells to B78 cells, a macrophage co-culture experiment was conducted with macrophages harvested from *Balb/c* mice. Unlike B78 cells (Fig. S4A), A20 tumor cells demonstrated significantly decreased proliferation when cultured in the presence of CpG (Fig. S4C). Adding macrophages, either *Balb/c* derived (Fig. S4C) or *C57BL/6* (not shown), to the culture did not further decrease proliferation. These in vitro and in vivo studies indicate CpG is functioning differently in the B78 and A20 models.

Systemic anti-tumor effect of CpG + OX40 decreases with increasing systemic A20 tumor burden

Using three separate two-tumor A20 models that varied in tumor volume, we investigated the strength of the systemic anti-tumor response of CpG + OX40 in the setting of increased systemic tumor burden. In one experiment in this model (~ 100 mm³ per tumor), CpG alone and OX40 alone were tested to validate the results others have published with these drugs in this model (Fig. S5). Similar to what others have described [17], CpG alone had a strong local anti-tumor effect but failed to slow distant, untreated tumor progression. OX40 alone slowed local and distant tumor progression, but CpG + OX40 demonstrated the strongest anti-tumor effect at both the local and distant tumors (Fig. S5). In the small two-tumor model (~ 100 mm³ per tumor),

once, intratumorally, with 50 μ g of CpG and all three tumor groups were harvested together, 48 h after CpG injection. P values calculated via one-way ANOVA analysis with Tukey's multiple comparison correction. * $P \leq 0.05$; ** $P \leq 0.01$; *** $P \leq 0.001$; **** $P \leq 0.0001$; ns, not significant

CpG + OX40 had a significant anti-tumor effect at both the treated and untreated tumors (Fig. 4a, b). CpG + OX40 significantly prolonged survival over PBS, and 70% of mice were cured (Fig. 4c, j, k).

In the moderate (~ 200 mm³ per tumor) two-tumor model, CpG + OX40 was effective at causing local tumor regression (Fig. 4d); however, after controlling distant tumor progression early in the experiment (days 3–18), tumor growth increased rapidly after day 18 (Fig. 4e). CpG + OX40 significantly prolonged survival compared to PBS in this moderate sized (~ 200 mm³) two-tumor model (Fig. 4f); however, 8 of 9 mice died of tumor progression before day 40.

In the large two-tumor model (~ 350 mm³ per tumor), the local tumor curing effects of CpG + OX40 observed with small tumors were significantly decreased (Fig. 4g, j), and there was no significant slowing of distant tumor progression (Fig. 4h). CpG + OX40 did maintain a small but significant prolongation of survival over PBS in this model (Fig. 4i), but no mice were cured with CpG + OX40 (Fig. 4j–k). As tumor burden increased, CpG + OX40 induced a significantly smaller percentage of local complete responses at the treated and untreated tumors (Fig. 4j–k).

Differing requirements of T cells for local and systemic anti-tumor response in small and large two-tumor A20 models

Given the varying effects of CpG + OX40 in the small and large two-tumor models (Fig. 4), we next tested the requirement of T cells following CpG + OX40 in T cell depletion studies.

In the small two-tumor model (~ 100 mm³), depleting CD4+ and CD8+ T cells did not prevent CpG + OX40 from significantly inhibiting local tumor progression (Fig. 5a). In the absence of T cells, CpG + OX40 lost its ability to control distant, untreated tumor progression (Fig. 5b), and the

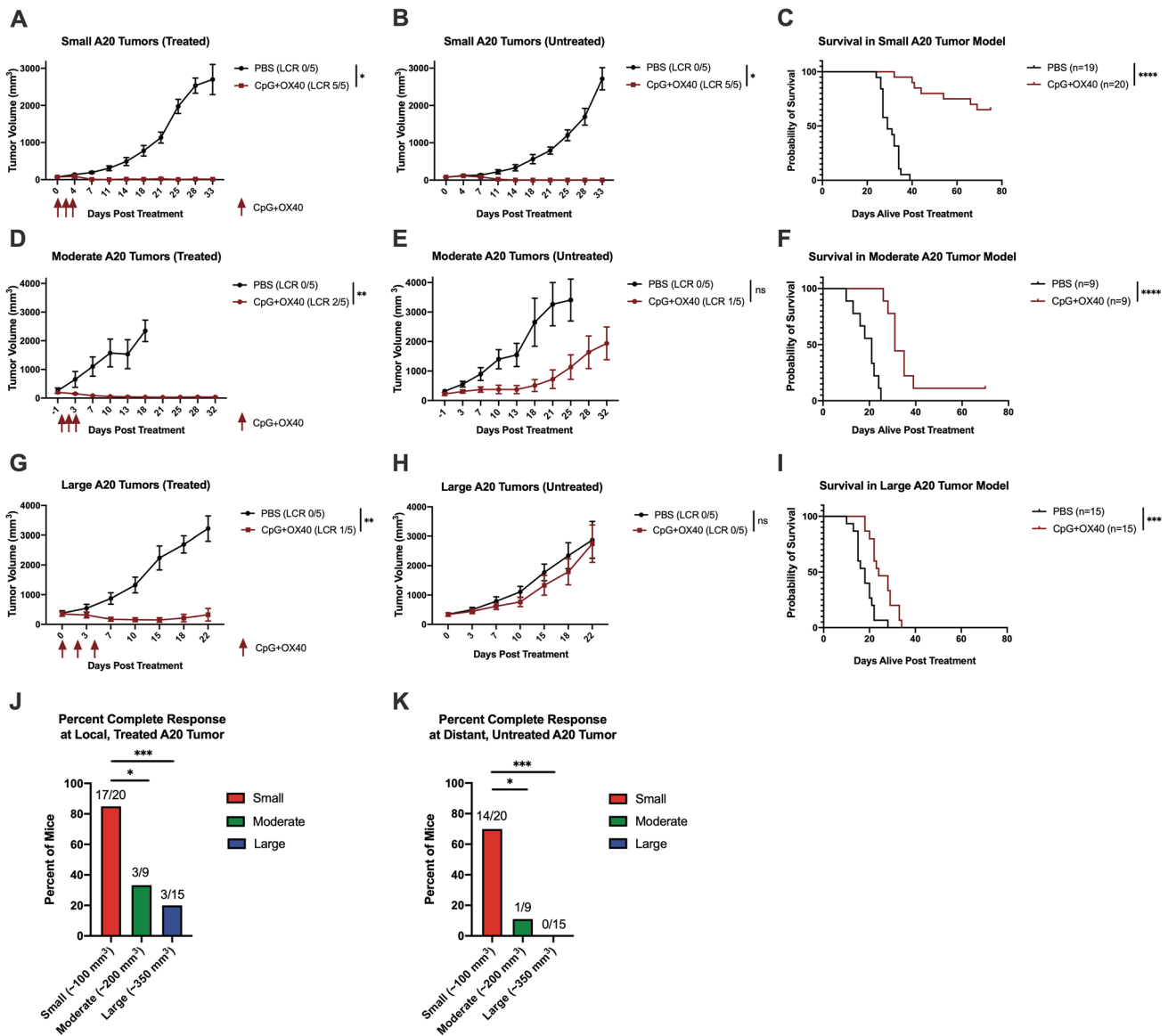


Fig. 4 Systemic in-situ vaccination strength decreases with increased systemic A20 tumor burden. *Balb/c* mice bearing 2 separate A20 tumors [(a–c) small (~100 mm³), (d–f) moderate (~200 mm³), and (g–i) large (~350 mm³) were treated with PBS (black) or CpG+OX40 (red). Average tumor volume (±SEM) are shown for the treated tumor (a, d, g), and the distant untreated tumor (b, e, h). The combined overall survival for each group is shown (c, f, i), using data pooled from at least 2 experiments. The number of mice demonstrating a local complete response (LCR) at the treated tumor or LCR specifically at the distant untreated tumor are shown in paren-

theses in (a, d, g) and (b, e, h), respectively. The percent of mice from combined experiments bearing small (red), moderate (green), or large (blue) tumors that demonstrated a LCR to CpG+OX40 at the (j) local, treated tumor and (k) distant, untreated tumor. P values for tumor volume plots were calculated using time-weighted average analysis. P values for overall survival were calculated via log rank test. P values for complete response data calculated via chi-square tests. *P ≤ 0.05; **P ≤ 0.01; ***P ≤ 0.001; ****P ≤ 0.0001; ns, not significant. All comparisons that are not shown with a *, **, *** or **** are not significantly different from each other

cohort of mice receiving T cell depletion were euthanized at a similar rate as the PBS control (Fig. 5c).

In the large two-tumor model (~100 mm³), mice in the CpG+OX40 and T cell depletion cohort demonstrated local tumor progression (Fig. 5d). At the distant, untreated tumors, all cohorts demonstrated a similar lack

of anti-tumor effect (Fig. 5e). Although the treatment with CpG+OX40 and IgG significantly prolonged survival (Fig. 5f), the effect was weaker than for the small tumor model (Fig. 5c), with all treated animals dying before day 40.

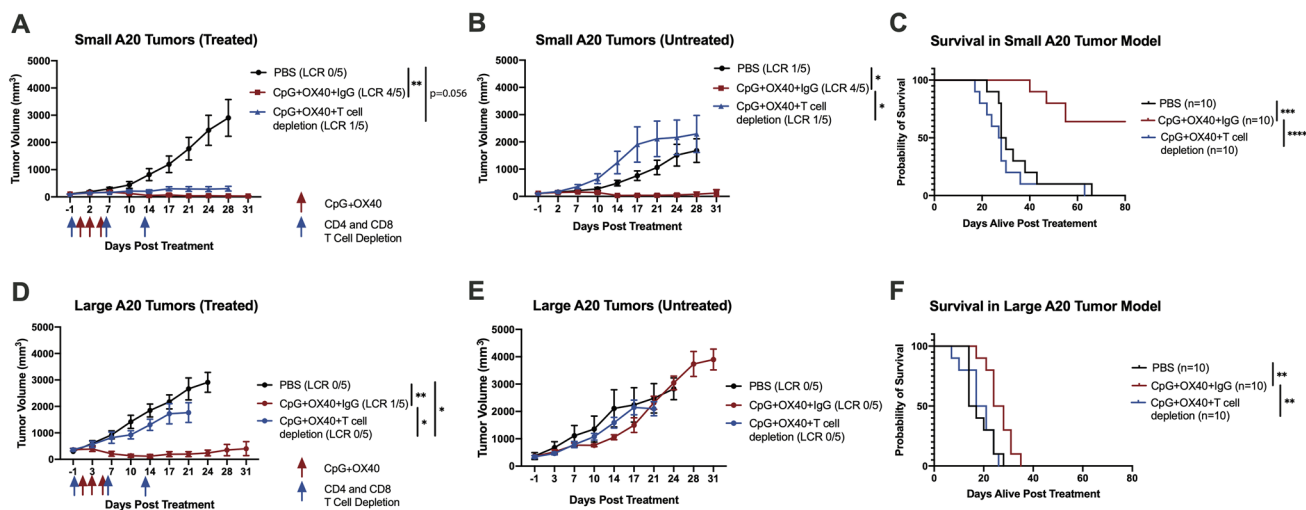


Fig. 5 Differing requirements of T cells for local anti-tumor response in small and large two-tumor A20 models. Representative average tumor volume (\pm SEM) of the **a, d** local, treated tumor, **b, e** distant, untreated tumor, and **c, f** overall survival from two independent experiments of mice treated with PBS (black), CpG + OX40 + Rat IgG (red), or CpG + OX40 + CD4 depletion + CD8 depletion (blue) in the (**a–c**) small ($\sim 100 \text{ mm}^3$) and (**d–f**) large ($\sim 350 \text{ mm}^3$) two-tumor A20 models. The number of mice demon-

strating a local complete response (LCR) at the treated tumor or distant untreated tumor are shown in parentheses in (**a, d**) and (**b, e**), respectively. *P* values for tumor volume plots were calculated using time-weighted average analysis. *P* values for overall survival were calculated via log rank test. **P* ≤ 0.05 ; ***P* ≤ 0.01 ; ****P* ≤ 0.001 ; *****P* ≤ 0.0001 . All comparisons that are not shown with an *, **, *** or **** are not significantly different from each other

Effects of systemic anti-CTLA-4 to CpG + OX40 in poorly responsive tumor models

After establishing that the CpG + OX40-induced distant anti-tumor effect was T cell dependent (Fig. 5b) and CD19⁺ cells in large A20 tumors express decreased CD80 and CD86 (Fig. 3), we hypothesized the addition of anti-CTLA-4 would augment T cell activation and enhance the anti-tumor effect of CpG + OX40 in the poorly responsive, large two-tumor A20 model given that CD80/86 are involved in T cell activation through the CD28/CTLA-4 axis [31]. Furthermore, we have previously shown additional Treg depletion via anti-CTLA-4 (IgG2a isotype) enables augmented cure rates in mice bearing larger B78 tumors that are no longer responding to a separate *in-situ* vaccine [radiation therapy (RT) + IT-IC] [14, 32]. Thus, we randomized mice bearing either a poorly responsive small ($\sim 100 \text{ mm}^3$) B78 tumor or two large ($\sim 350 \text{ mm}^3$ per tumor) A20 tumors into 4 treatment groups: PBS, anti-CTLA-4, CpG + OX40, and CpG + OX40 + anti-CTLA-4.

In the small B78 model, the addition of anti-CTLA-4 to CpG + OX40 had no effect on slowing tumor progression or overall survival (Fig. 6a, b). In the large two-tumor A20 model, the addition of anti-CTLA-4 to CpG + OX40 caused significant local tumor regression compared to PBS and anti-CTLA-4 alone and caused regression of some tumors at the distant untreated site (LCR 5 of 10 at the treated tumor and 4 of 10 at the distant tumor) (Fig. 6c, d, f, g).

CpG + OX40 + anti-CTLA-4 significantly improved survival over all other groups in these studies; 40% of mice treated with CpG + OX40 + anti-CTLA-4 were cured, while all mice in all other groups died before day 40 (Fig. 6e).

Discussion

Herein, we demonstrate tumor volume is a critical variable for CpG + OX40 sensitivity in both the B78 and A20 tumor models. While first-palpable ($\sim 15 \text{ mm}^3$) B78 tumors respond well to CpG + OX40, 100 mm^3 B78 tumors do not; in contrast, single 200 or 350 mm^3 A20 tumors respond well to CpG + OX40 while single 1000 mm^3 A20 tumors partially respond before progressing. Similar relationships between tumor volume and systemic response to CpG + OX40 are demonstrated in our two-tumor A20 model. While the pre-clinical tumor volumes presented in this study do not directly correlate to patient clinical tumor sizes, we believe the general relationship between anti-tumor effect and tumor size shown in this study correlates with some published clinical observations [1–5, 8]. Our preclinical results support the retrospective studies that have examined the relationship of patient tumor burden and response to immune checkpoint blockade in melanoma and non-small cell lung cancer [1–3]. Additionally, the data highlight the importance of considering tumor size when immunotherapy treatment is initiated in preclinical models. Most curative preclinical immunotherapy

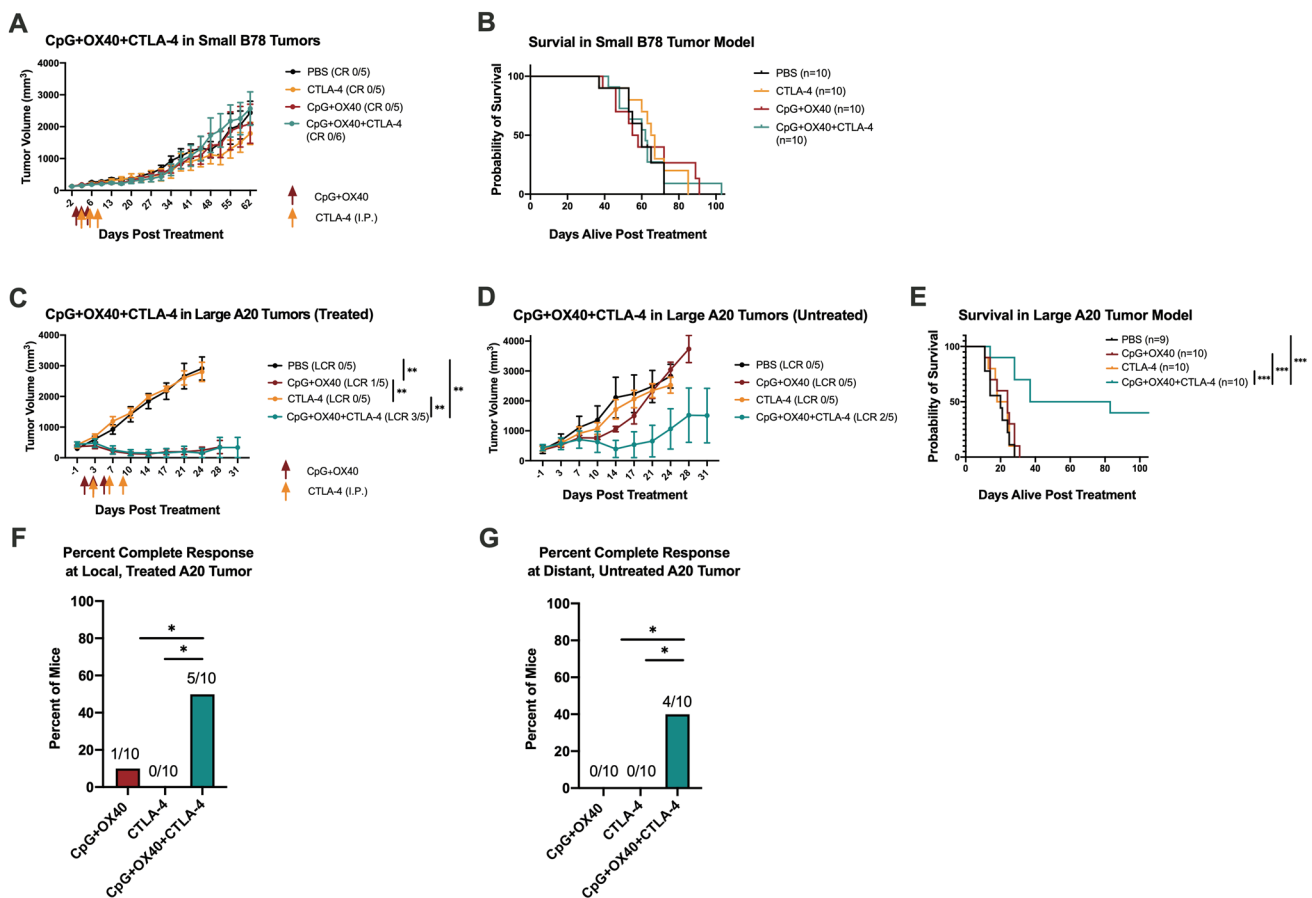


Fig. 6 Anti-CTLA-4 enhances the anti-tumor response of CpG+OX40 in the poorly responsive A20 but not B78 tumor models. **a** Average tumor volume (\pm SEM) from a representative experiment and **b** combined overall survival from two independent experiments in *C57BL/6* mice bearing a single small (~ 100 mm³) B78 flank tumor treated with PBS (black), anti-CTLA-4 (yellow), CpG+OX40 (red), or CpG+OX40+anti-CTLA-4 (teal). **c** Average tumor volume (\pm SEM) plot of the local, treated tumor and **d** distant, untreated tumor from a representative experiment, and **e** combined overall survival from two independent experiments of *Balb/c* mice treated with PBS (black), anti-CTLA-4 (yellow), CpG+OX40 (red), or CpG+OX40+anti-CTLA-4 (teal) in mice bearing two separate large (~ 350 mm³) A20 tumors. [Note in Fig. 6C, the data

for CpG+OX40+anti-CTLA-4 (teal) are superimposed on the data for CpG+OX40 (red), making it hard to view]. The number of mice demonstrating a local complete response (LCR) at the treated tumor or distant untreated tumor are shown in parentheses in (**a**, **c**) and (**d**), respectively. Percent of *Balb/c* mice treated with CpG+OX40 (red), anti-CTLA-4 (yellow), or CpG+OX40+anti-CTLA-4 (teal) cured of their local, treated A20 tumor (**f**) and distant, untreated A20 tumor (**g**). *P* values for tumor volume plots were calculated using time-weighted average analysis. *P* values for overall survival were calculated via log rank test. *P* values for CR comparison calculated via chi-square tests. **P* ≤ 0.05 ; ***P* ≤ 0.01 ; ****P* ≤ 0.001 . All comparisons that are not shown with an *, **, or *** are not significantly different from each other

regimens are tested when tumors are less than 200 mm³ and/or have been growing for less than 11 days in the host [33]. The data examined in the context of time in the host before treatment aligns well with these generalized conclusions. Specially, B78 tumors growing in the host were significantly more likely to respond to CpG+OX40 if they had been growing for 10 days (first palpable, 15 mm³) rather than 21 days (small, 100 mm³) (Fig. 1e). In the A20 model, tumors growing in their host for 24 days (advanced, $\sim 1,000$ mm³) were less responsive than those growing for 14 days (moderate, ~ 200 mm³) (Fig. 2e). Our data suggest that more time in the host allows for more tumor growth and more immunoeediting (potentially of the tumor cells or of the

tumor microenvironment), and thus leads to more difficult to treat tumors (e.g. decreased MHC-I, MHC-II, and CD80/86 expression in large A20 tumors shown here) (Fig. 3a–c). However, this manuscript does not specifically address how the antitumor effect of CpG+OX40 is influenced by the time since implantation vs. tumor size at the time treatment is initiated. In prior work we have shown that the potency of the response of B78 tumors to treatment with intratumoral hu14.18-IL2 immunocytokine following local radiotherapy was the same for tumors of the same size, even when the time to treatment was somewhat different [34].

When syngeneic tumor cells are injected into mice, acute inflammation and necrosis occur at the injection site. This

is followed by cross-presentation and antigen priming, potentially resulting in some baseline anti-tumor immune response [33]. As syngeneic tumors progress, the baseline anti-tumor immune response dampens due to immunoeediting and tumor immune suppression [6, 8]. As a result, an immunotherapy regimen could be inaccurately deemed a preclinical success or failure based on when immunotherapy is initiated, how large tumors are at the start of treatment, and what preclinical model is used. In addition to the extent of tumor burden, local and systemic immunologic changes that occur with tumor progression can suppress the anti-tumor effects of immunotherapy [35, 36]. Here, we show A20 tumors decrease MHC class I and II, CD80, and CD86 expression with progression. While most clinical trials of immunotherapy regimens are based on preclinical success, many of these clinical trials do not replicate the successful preclinical anti-tumor effects. Given the financial and human costs associated with the development and performance of these clinical trials [37–39], it may be helpful to confirm preclinical regimens demonstrate efficacy across multiple tumor models, and in tumors of various sizes, when considering whether to translate these regimens to clinical testing.

We have previously published different *in vivo* responses to CpG between the B78 and A20 models [25]. Specifically, CpG increases OX40 expression on CD8 + T cells and CD4 + non-Tregs in the TME of A20 tumors but not B78 tumors [25]. Our data presented in this report suggest CpG is working in the B78 model to activate tumor infiltrating macrophages, which agrees with previous publications that indicate CpG activates anti-tumor macrophages via IFN-dependent pathways [40]. In the A20 model, CpG has direct anti-proliferative effects against A20 tumor cells and alters A20 tumor phenotype both *in vitro* and *in vivo*. OX40 antibody appears to function in both A20 and B78 models, in part, by decreasing tumor Treg frequency [16]. Therefore, the difference in CpG activity between the B78 and A20 models might contribute to the relative volume differences seen in the CpG + OX40 response between these two models. Clearly other factors are likely involved in this differential response, possibly including the immune capabilities of *C57BL/6* and *Balb/c* mice and the higher immunogenicity of A20 lymphoma compared to B78 melanoma.

Investigation into the role of myeloid derived suppressive cells (MDSCs), not only in the context of tumor progression, but also the response to CpG + OX40 *in-situ* vaccination is an area of future interest. Some studies have demonstrated that increased levels of MDSCs negatively correlate with outcomes in patients diagnosed with cancer, including melanoma and lymphoma [41–43]. Preclinical studies have shown that MDSC accumulation in the TME significantly increases as tumor volumes increase [6]. The effects of CpG on MDSCs have been characterized in mice bearing two types of gastrointestinal tumors (C26 and CEA424-TAG

models) [44]. In these experiments, CpG was shown to decrease the suppressive potential of systemic MDSCs against T cells, and this mechanism was dependent on IFN- α . While MDSCs were not examined in this manuscript, we suggest that future studies evaluate whether systemic, or tumor associated, MDSC frequencies are higher in model conditions that are less responsive to the CpG + OX40 *in-situ* vaccine, and whether IT injections of CpG + OX40 may act to decrease the suppressive potential of MDSCs allowing a measurable anti-tumor immune response under some model conditions.

In the A20 model, CpG + OX40 effectively cured mice bearing a single large ($\sim 350 \text{ mm}^3$) flank tumor. If, however, a mouse had a second, similarly sized, untreated tumor on the opposite flank, the ability of CpG + OX40 to cure the local $\sim 350 \text{ mm}^3$ treated tumor was reduced (Fig. 2d, E vs Fig. 4g,i). Concomitant immune tolerance (CIT) is a possible explanation for the reduced local efficacy. CIT is a phenomenon describing tumor specific inhibition of *in-situ* vaccination by distant untreated tumor sites [32]. We have previously observed CIT in the two-tumor B78 model in the context of treatment with RT and IT-IC [32]. Those studies suggest that after Treg depletion with RT to the local tumor, Tregs from the distant untreated tumor repopulate these treated tumors, inhibiting the response to immunotherapy [32]. Others have published data in the two-tumor A20 model demonstrating that Tregs can migrate from one tumor to another [16]. It is possible Tregs from large, untreated A20 tumors are migrating to the treated tumor, reducing the ability of CpG + OX40 to activate a tumor-curing immune response.

In mice bearing $\sim 100 \text{ mm}^3$ B78 tumors, the addition of anti-CTLA-4 causes a decrease in Tregs and an increase in T cell activation [32]; even so, the addition of anti-CTLA-4 failed to improve the anti-tumor response of CpG + OX40. We have previously reported that additional T cell activation in the form of increasing OX40 dose fails to augment the anti-tumor response in the B78 model [25]. These results suggest Treg immune suppression and inadequate T cell activation are not responsible for the failed effect of CpG + OX40 in the $\sim 100 \text{ mm}^3$ B78 model. Instead, we hypothesize CpG + OX40 is failing to initiate a strong anti-tumor immune reaction, and thus additional immune stimulation is required. We have previously demonstrated RT can provide this additional immune activation to CpG + OX40 in ~ 100 – 150 mm^3 B78 tumors by increasing IFN gene expression in the TME, increasing OX40 expression on tumor infiltrating CD4 + T cells, and increasing IFN- γ expression in CD8 + and CD4 + T cells in the tumor draining lymph node (TDLN) and spleen [25]. Conversely, additional Treg depletion via anti-CTLA-4 in the A20 model enhances both the local and systemic anti-tumor effects of CpG + OX40. This agrees with previous work on this *in-situ*

vaccine in the A20 model [16]. However, our data demonstrating decreased MHC-I, MHC-II, CD80, and CD86 expression as A20 tumors progress provide additional context to the mechanism of this enhanced anti-tumor response. CD80 and CD86 are T cell co-stimulatory molecules on APCs that interact with CD28 or CTLA-4 on T cells, providing either a positive (CD28 binding) or attenuated (CTLA-4 binding) costimulatory signal to the T cell when a T cell receptor engages MHC on APCs. This axis is typically examined in the context of secondary lymphoid organs during T cell priming [31, 45]. Emerging evidence suggest this axis (e.g., CD80/86, CD28/CTLA-4) is also important outside the context of initial T cell priming and activation, demonstrating that CD4+ effector cells require sustained CD28 signaling to generate a proper type I helper response [46]. It is possible downregulated CD80 and CD86 expression in large A20 tumors is preventing the sustained CD28 signaling required for an effective adaptive anti-tumor response. Whether additional injections of CpG + OX40 (e.g. 4 or more) would overcome inhibitory effects in non-responsive models, potentially through additional CD80/86 expression changes, or increased antigen presentation, is an area of future interest. In a separate study, 9 injections of an in-situ vaccine, consisting of a STING agonist and an anti-GITR antibody, failed to improve the anti-tumor response in a two-tumor A20 model over 3 injections of the in-situ vaccine [47].

As immunotherapy continues to become part of standard of care, it will be important to better understand how tumor type and tumor burden impact the efficacy and mechanism of immunotherapy treatments. Tumor size is a criterion for the American Joint Committee on Cancer tumor staging in many cancer types, influencing treatment decisions with traditional cancer treatment modalities (i.e., RT, chemotherapy, and surgery). Emerging clinical and preclinical data, including this report, indicate tumor size and number of tumors may need to be considered when prescribing immunotherapy regimens [1–3, 7, 14, 27].

Conclusion

The preclinical data presented here demonstrate the negative impact larger tumor burdens have on the efficacy and mechanism of CpG + OX40 *in-situ* vaccine in two separate tumor models. For comparably sized tumors, B78 melanoma was less responsive to CpG + OX40 than A20 lymphoma, and differences of these tumors' response to CpG may, in part, account for these differences to the treatment. Anti-CTLA-4 antibody, although not effective by itself against larger tumors, can restore the anti-tumor efficacy of CpG + OX40 in larger A20 lymphomas but not in larger B78 melanomas. Our findings suggest parameters such as tumor type and

tumor volume should be carefully considered when designing and testing immunotherapy regimens in preclinical settings to better predict potential clinical activity.

Supplementary Information The online version contains supplementary material available at <https://doi.org/10.1007/s00262-023-03433-3>.

Acknowledgements We appreciate the thoughtful discussions and conversations surrounding results and implications with Dr. Ravi B. Patel. We are thankful for support and suggestions provided by Dr. Stephen D. Gillies regarding the A20 cell line and A20 *in vivo* growth. We are grateful for the assistance from UWCCC Flow Cytometry Laboratory, which is supported by the University of Wisconsin Carbone Cancer Center Support Grant P30 CA014520.

Authors' contributions AAP, DVS, ALR, PMS were responsible for experimental design, execution, and analysis of data. AAP created final versions of all figures and drafted the manuscript. AAP, DVS, MARF, ASF, and NWT collected and analyzed experimental data. AAP, DVS, NWT, ASF collected tissue for flow cytometry analysis. JZ conducted and confirmed statistical analysis of experimental data. PMS, ALR, AKE, and ZSM contributed to experimental design, thorough edits, and review of the manuscript. ALR, MARF, and AKE contributed to experimental design, data collection, mouse colony maintenance, and literature research. All authors provided thorough review and editing of the manuscript draft.

Funding This work was supported by Midwest Athletes Against Childhood Cancer; Stand Up 2 Cancer; the St. Baldrick's Foundation; the Crawdaddy Foundation; and the University of Wisconsin Carbone Cancer Center. This research was also supported in part by public health service grants TR002373, U54-CA232568, R35-CA197078, 1DP5OD024576, U01-CA233102, P50 DE026787, P01 CA250972 from the National Cancer Institute; the National Institutes of Health and the Department of Health and Human Services. AAP was supported by NIH awards TL1 TR002375 and T32 GM140935. Additional support was provided by the Clinical and Translational Science Award (CTSA) program, through the NIH National Center for Advancing Translational Sciences (NCATS), grant UL1TR000427. The content is solely the responsibility of the authors and does not necessarily represent the official views of the National Institutes of Health.

Data Availability For information regarding the data presented in this work, please contact the Corresponding Author at pmsondel@humonc.wisc.edu.

Declarations

Conflict of interest ZSM is a member of the scientific advisory board for Archeus Technologies and Seneca Therapeutics and received equity options for these companies. ZSM is an inventor on patents or filed patents managed by the Wisconsin Alumni Research Foundation relating to the interaction of targeted radionuclide therapies and immunotherapies, nanoparticles designed to augment the anti-tumor immune response following radiation therapy, and the development of a brachytherapy catheter capable of delivering intra-tumor injectables. PMS is an inventor on patents or filed patents managed by the Wisconsin Alumni Research Foundation relating to mAb-related immunotherapies and the interaction of targeted radionuclide therapies and immunotherapies.

Ethical approval The research contained in this manuscript does not utilize patient data in any form. Animal studies were conducted according to a protocol approved by the University of Wisconsin Institutional Animal Care and Use Committee.

Consent to Publish All listed coauthors have provided their consent for publication of this work, and attest that it has not been previously published in manuscript form.

Open Access This article is licensed under a Creative Commons Attribution 4.0 International License, which permits use, sharing, adaptation, distribution and reproduction in any medium or format, as long as you give appropriate credit to the original author(s) and the source, provide a link to the Creative Commons licence, and indicate if changes were made. The images or other third party material in this article are included in the article's Creative Commons licence, unless indicated otherwise in a credit line to the material. If material is not included in the article's Creative Commons licence and your intended use is not permitted by statutory regulation or exceeds the permitted use, you will need to obtain permission directly from the copyright holder. To view a copy of this licence, visit <http://creativecommons.org/licenses/by/4.0/>.

References

- Chardin D, Paquet M, Schiappa R et al (2020) Baseline metabolic tumor volume as a strong predictive and prognostic biomarker in patients with non-small cell lung cancer treated with PD1 inhibitors: a prospective study. *J Immunother Cancer* 8(2).
- Joseph RW, Elassaiss-Schaap J, Kefford R et al (2018) Baseline tumor size is an independent prognostic factor for overall survival in patients with melanoma treated with pembrolizumab. *Clin Cancer Res* 24(20):4960–4967
- Katsurada M, Nagano T, Tachihara M et al (2019) Baseline tumor size as a predictive and prognostic factor of immune checkpoint inhibitor therapy for non-small cell lung cancer. *Anticancer Res* 39(2):815–825
- Guisier F, Cousse S, Jeanvoine M et al (2019) A rationale for surgical debulking to improve anti-PD1 therapy outcome in non small cell lung cancer. *Sci Rep* 9(1):16902
- Nessler JP, Lee MH, Nguyen C et al (2020) Tumor size matters—understanding concomitant tumor immunity in the context of hypofractionated radiotherapy with immunotherapy. *Cancers (Basel)* 12(3).
- Yu JW, Bhattacharya S, Yanamandra N et al (2018) Tumor-immune profiling of murine syngeneic tumor models as a framework to guide mechanistic studies and predict therapy response in distinct tumor microenvironments. *PLoS ONE* 13(11):e0206223
- Yang RK, Kalogriopoulos NA, Rakhmievich AL et al (2013) Intratumoral treatment of smaller mouse neuroblastoma tumors with a recombinant protein consisting of IL-2 linked to the hu14.18 antibody increases intratumoral CD8+ T and NK cells and improves survival. *Cancer Immunol Immunother* 62(8):1303–1313.
- Kim SI, Cassella CR, Byrne KT (2020) Tumor burden and immunotherapy: impact on immune infiltration and therapeutic outcomes. *Front Immunol* 11:629722
- Gajewski TF (2015) The next hurdle in cancer immunotherapy: overcoming the non-T-cell-inflamed tumor microenvironment. *Semin Oncol* 42(4):663–671
- Schakenraad A, Hashemi S, Twisk J et al (2021) The effect of tumor size and metastatic extent on the efficacy of first line pembrolizumab monotherapy in patients with high PD-L1 expressing advanced NSCLC tumors. *Lung Cancer* 162:36–41
- French RR, Chan HT, Tutt AL et al (1999) CD40 antibody evokes a cytotoxic T-cell response that eradicates lymphoma and bypasses T-cell help. *Nat Med* 5(5):548–553
- Albertini MR, Yang RK, Ranheim EA et al (2018) Pilot trial of the hu14.18-IL2 immunocytokine in patients with completely resectable recurrent stage III or stage IV melanoma. *Cancer Immunol Immunother* 67(10):1647–1658.
- Yang, RK, Kalogriopoulos NA, Rakhmievich AL et al (2012) Intratumoral hu14.18-IL-2 (IC) induces local and systemic anti-tumor effects that involve both activated T and NK cells as well as enhanced IC retention. *J Immunol* 189(5):2656–2664.
- Morris ZS, Guy EI, Francis DM et al (2016) In situ tumor vaccination by combining local radiation and tumor-specific antibody or immunocytokine treatments. *Cancer Res* 76(13):3929–3941
- Houot, R and R Levy, T-cell modulation combined with intratumoral CpG cures lymphoma in a mouse model without the need for chemotherapy. *Blood*, 2009. 113(15): p. 3546–52.
- Marabelle A, Kohrt H, Sagiv-Barfi I et al (2013) Depleting tumor-specific Tregs at a single site eradicates disseminated tumors. *J Clin Invest* 123(6):2447–2463
- Sagiv-Barfi I, Czerwinski DK, Levy S et al (2018) Eradication of spontaneous malignancy by local immunotherapy. *Sci Transl Med* 10(426).
- Karapetyan L, Luke JJ, Davar D (2020) Toll-like receptor 9 agonists in cancer. *Onco Targets Ther* 13:10039–10060
- al-Shamkhani A, Birkeland ML, Puklavec M et al (1996) OX40 is differentially expressed on activated rat and mouse T cells and is the sole receptor for the OX40 ligand. *Eur J Immunol* 26(8):1695–1659
- Gramaglia I, Jember A, Pippig SD et al (2000) The OX40 costimulatory receptor determines the development of CD4 memory by regulating primary clonal expansion. *J Immunol* 165(6):3043–3050
- Croft M (2010) Control of immunity by the TNFR-related molecule OX40 (CD134). *Annu Rev Immunol* 28:57–78
- Vu MD, Xiao X, Gao W et al (2007) OX40 costimulation turns off Foxp3+ Tregs. *Blood* 110(7):2501–2510
- Ito T, Wang YH, Duramad O et al (2006) OX40 ligand shuts down IL-10-producing regulatory T cells. *Proc Natl Acad Sci U S A* 103(35):13138–13143
- Bulliard Y, Jolicoeur R, Zhang J et al (2014) OX40 engagement depletes intratumoral Tregs via activating FcγR2b, leading to antitumor efficacy. *Immunol Cell Biol* 92(6):475–480
- Pieper AA, Zangl LM, Spiegelman DV et al (2021) Radiation augments the local anti-tumor effect of in situ vaccine with CpG-oligodeoxynucleotides and anti-OX40 in immunologically cold tumor models. *Front Immunol* 12:763888
- Rakhmievich AL, Felder M, Lever L et al (2017) Effective combination of innate and adaptive immunotherapeutic approaches in a mouse melanoma model. *J Immunol* 198(4):1575–1584
- Pieper AA, Rakhmievich AL, Spiegelman DV et al (2021) Combination of radiation therapy, bempagedesleukin, and checkpoint blockade eradicates advanced solid tumors and metastases in mice. *J Immunother Cancer* 9(6).
- Buhtoiarov IN, Lum HD, Berke G et al (2006) Synergistic activation of macrophages via CD40 and TLR9 results in T cell independent antitumor effects. *J Immunol* 176(1):309–318
- Li J, Song W, Czerwinski DK et al (2007) Lymphoma immunotherapy with CpG oligodeoxynucleotides requires TLR9 either in the host or in the tumor itself. *J Immunol* 179(4):2493–2500
- Jahrsdorfer B, Hartmann G, Racila E et al (2001) CpG DNA increases primary malignant B cell expression of costimulatory molecules and target antigens. *J Leukoc Biol* 69(1):81–88
- Qureshi OS, Zheng Y, Nakamura K et al (2011) Trans-endocytosis of CD80 and CD86: a molecular basis for the cell-extrinsic function of CTLA-4. *Science* 332(6029):600–603
- Morris ZS, Guy EI, Werner LR et al (2018) Tumor-specific inhibition of in situ vaccination by distant untreated tumor sites. *Cancer Immunol Res* 6(7):825–834

33. Schreiber K, Rowley DA, Riethmüller G et al (2006) Cancer immunotherapy and preclinical studies: why we are not wasting our time with animal experiments. *Hematol Oncol Clin North Am* 20(3):567–584
34. Carlson PM, Mohan M, Rodriguez M et al (2021) Depth of tumor implantation affects response to in situ vaccination in a syngeneic murine melanoma model. *J Immunother Cancer* 9(4).
35. Lin, JH, Huffman AP, Wattenberg MM et al (2020) Type 1 conventional dendritic cells are systemically dysregulated early in pancreatic carcinogenesis. *J Exp Med* 217(8).
36. Allen BM, Hiam KJ, Burnett CE et al (2020) Systemic dysfunction and plasticity of the immune macroenvironment in cancer models. *Nat Med* 26(7):1125–1134
37. Johnson JI, Decker S, Zaharevitz D et al (2001) Relationships between drug activity in NCI preclinical in vitro and in vivo models and early clinical trials. *Br J Cancer* 84(10):1424–1431
38. Adams CP, Brantner VV (2006) Estimating the cost of new drug development: is it really 802 million dollars? *Health Aff (Millwood)* 25(2):420–428
39. Sharpless NE, Depinho RA (2006) The mighty mouse: genetically engineered mouse models in cancer drug development. *Nat Rev Drug Discov* 5(9):741–754
40. Buhtoiarov IN, Sondel PM, Eickhoff JC et al (2007) Macrophages are essential for antitumour effects against weakly immunogenic murine tumours induced by class B CpG-oligodeoxynucleotides. *Immunology* 120(3):412–423
41. Weide B, Martens A, Zelba H et al (2014) Myeloid-derived suppressor cells predict survival of patients with advanced melanoma: comparison with regulatory T cells and NY-ESO-1- or melan-A-specific T cells. *Clin Cancer Res* 20(6):1601–1609
42. Betsch A, Rutgeerts O, Fevery S et al (2018) Myeloid-derived suppressor cells in lymphoma: the good, the bad and the ugly. *Blood Rev* 32(6):490–498
43. Wang PF, Song SY, Wang TJ et al (2018) Prognostic role of pre-treatment circulating MDSCs in patients with solid malignancies: a meta-analysis of 40 studies. *Oncoimmunology* 7(10):e1494113
44. Zoglmeier C, Bauer H, Noerenberg D et al (2011) CpG blocks immunosuppression by myeloid-derived suppressor cells in tumor-bearing mice. *Clin Cancer Res* 17(7):1765–1775
45. Wei SC, Duffy CR, Allison JP (2018) Fundamental mechanisms of immune checkpoint blockade therapy. *Cancer Discov* 8(9):1069–1086
46. Linterman MA, Denton AE, Divekar DP et al (2014) CD28 expression is required after T cell priming for helper T cell responses and protective immunity to infection. *Elife*, 3.
47. Sallets A, Robinson S, Kardosh A et al (2018) Enhancing immunotherapy of STING agonist for lymphoma in preclinical models. *Blood Adv* 2(17):2230–2241

Publisher's Note Springer Nature remains neutral with regard to jurisdictional claims in published maps and institutional affiliations.